Evolution of Midgap States and Residual Three Dimensionality in $La_{2-x}Sr_xCuO_4$

S. Sahrakorpi,[1] M. Lindroos,[1,2] R. S. Markiewicz,[1] and A. Bansil[1]

[1]*Physics Department, Northeastern University, Boston, Massachusetts 02115, USA*

[2]*Institute of Physics, Tampere University of Technology, P.O. Box 692, 33101 Tampere, Finland*

(Received 19 January 2005; published 4 October 2005)

We carry out extensive first-principles doping-dependent computations of angle-resolved photoemission (ARPES) intensities in $La_{2-x}Sr_xCuO_4$ over a wide range of binding energies. Intercell hopping and the associated three dimensionality, which is usually neglected in discussing cuprate physics, is shown to play a key role in shaping the ARPES spectra. Despite the obvious importance of strong coupling effects (e.g., the presence of a lower Hubbard band coexisting with midgap states in the doped insulator), a number of salient features of the experimental ARPES spectra are captured to a surprising extent when k_z dispersion is properly included in the analysis.

DOI: 10.1103/PhysRevLett.95.157601 PACS numbers: 79.60.−i, 71.18.+y, 74.72.Dn

$La_{2-x}Sr_xCuO_4$ (LSCO) has drawn intense interest as a model system for understanding one of the most hotly debated issues in condensed matter physics currently, namely, how does a Mott insulator, La_2CuO_4 (LCO), develop into a superconductor when doped with holes, and what is the route taken by the electronic states in the insulator to achieve this remarkable transformation into a metal [1,2]. Angle-resolved photoemission spectroscopy (ARPES) has been brought to bear on these questions in recent years as techniques for preparing LSCO surfaces have improved [3–8]. ARPES spectra in LCO find a lower Hubbard band (LHB) associated with an insulating state, which persists with finite hole doping, losing intensity without shifting in energy. At the same time *new states*—the so-called midgap states—appear close to the Fermi level, which evolve into the conventional metallic bands near optimal doping. Doping-dependent ARPES spectra in LSCO thus address a wide range of issues concerning stripe and pseudogap physics and their relation to the mechanism of high-temperature superconductivity, and bear on questions of non-Fermi liquid behavior or gossamer superconductivity [9,10], among others [11].

We have recently shown with the example of $Bi_2Sr_2CaCu_2O_8$ (Bi2212) that the residual k_z dispersion of bands in a quasi-2D material will induce an irreducible linewidth in ARPES peaks, which is unrelated to any scattering mechanism [12]. This effect becomes accentuated in LSCO, where the bands possess a greater 3D character compared to Bi2212. This Letter reports extensive first-principles computations of the ARPES intensity in LSCO with the goal of ascertaining the extent to which k_z dispersion affects the experimental spectra of the midgap and LHB states. The interplay between the effects of the ARPES matrix element [13–15] and the k_z dispersion yields computed intensity maps for emission from the Fermi energy (E_F) as well as for binding energies several hundred meV below E_F, which are in surprising accord with the corresponding measurements.

Our calculations give insight into a number of salient features of the experimental spectra, such as the dispersion of the midgap states and the characteristic broadenings and symmetries or lack thereof in the photointensities. Evidence of physics beyond the framework of the conventional local-density approximation (LDA) based picture is especially clear in the strongly underdoped regime, both in the appearance of a d-wave-like pseudogap in the midgap states and in the presence of the LHB near half-filling. We discuss this insulating regime in terms of tight-binding (TB) computations, in which the LDA-inspired overlap parameters are supplemented with a Hubbard U or a pseudogap Δ. The effect of k_z dispersion is included through an intercell hopping parameter—to our knowledge for the first time in connection with a TB description of the cuprates. In this way, via comparisons between theory and experiment, we adduce a strong connection between the LDA generated metallic states and the evolution of the midgap band throughout the doping range.

With regard to relevant computational details, the fully self-consistent electronic structure of tetragonal LCO was obtained within the LDA by using the well-established all electron Green function methodology [16]; our band structure and Fermi surface (FS) are in accord with published data [17]. Following common practice, the metallic state of LSCO obtained by doping LCO with Sr is assumed to be described by a rigid band shift of the LDA generated metallic band structure of LCO. All presented ARPES intensities have been computed within the one-step photoemission formalism, assuming an LaO-layer terminated surface. The calculations properly model the photoemission process and take account of the associated dipole matrix element and its dependencies on photon energy and polarization; see Refs. [12–14] for details.

Figure 1 considers emission from E_F for optimally doped LSCO and shows the remarkable degree to which the FS map can be understood within the framework of the conventional LDA-based picture. We start by looking at the left side of panel (a), where the red filled region gives the projection of the 3D FS onto the (k_x, k_y) plane and encompasses various FS cross sections as a function of k_z [18]. Emission of photoelectrons is possible in principle

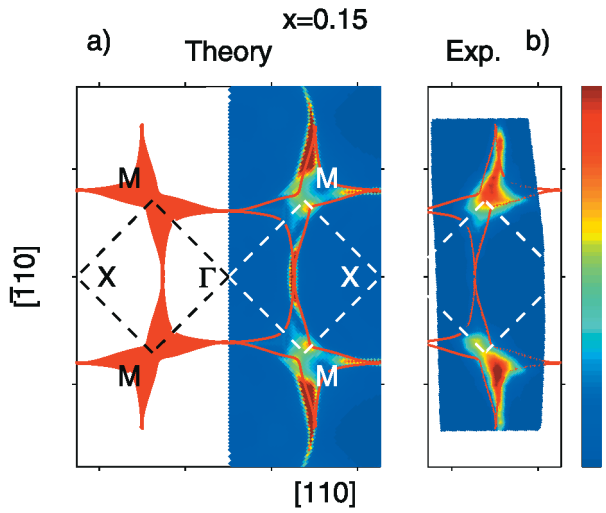

FIG. 1 (color). ARPES spectra for emission from the Fermi energy in optimally doped LSCO for $x = 0.15$. (a) Red filled region on left-hand side gives the 3D Fermi surface projected onto the (k_x, k_y) plane and denotes the area of allowed emissions. The right-hand side gives computed intensity including the effect of the ARPES matrix elements with red lines marking boundaries of the red filled regions. (b) Corresponding experimental spectra [4].

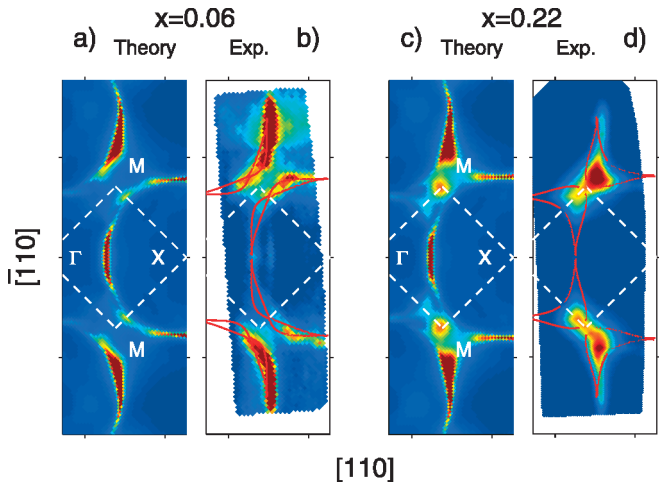

FIG. 2 (color). Similar to Fig. 1, except that this figure refers to the underdoped, $x = 0.06$ [panels (a) and (b) (Ref. [8])], and overdoped, $x = 0.22$ [panels (c) and (d) (Ref. [5])], cases.

from any part of this red region due to the quasi-2D nature of the states. (In a strictly 2D system, the red region will collapse into a standard FS contour of zero width.) We emphasize that the photointensity within this red region in general will not be uniform as it will be modified by the effect of the ARPES matrix element. This aspect is delineated on the right side of panel (a), where the theoretically predicted ARPES intensity is shown superposed with the boundaries of the region of allowed transitions by red lines. In comparing theoretical intensities in panel (a) with the experimental results [4,19] in panel (b), the most striking feature is the appearance of winglike structures around the antinodal points $M(\pi, 0)$ in both theory and experiment. On the other hand, along the nodal direction in the first Brillouin zone (BZ), Γ to $X(\pi, \pi)$, the high computed intensity is not reproduced in the measurements. However, we find that this computed nodal intensity is quite sensitive to photon energy. It will be necessary to carry out ARPES experiments over a range of photon energies in order to ascertain whether absence of nodal intensity represents a significant effect of correlations beyond the LDA in LSCO.

Figure 2 expands the preceding discussion to include the underdoped and overdoped regimes. The computations in all cases simulate experimental conditions [5,8,19]. The theory is seen to provide a good overall description of the data over the entire doping range, discrepancies along the nodal direction notwithstanding. In the underdoped sample the intensity is concentrated in two features lying above and below the M point. In contrast, the FS crosses the van Hove singularity (vHS) near optimal doping, and the overdoped sample displays a greater spectral weight around the M point. Since the midgap states evolve into conventional bands with increased doping, the good agreement with theory is perhaps to be expected in optimally and overdoped samples, but the continued agreement for the underdoped sample is quite remarkable—particularly since the midgap states have a pseudogap, as discussed below.

Figures 1 and 2 make it clear that the broadening of ARPES spectra resulting from the effect of k_z dispersion is essentially zero along the nodal direction and that it increases only gradually as one moves towards the antinodal region. By contrast, in the antinodal region, the combined effects of the vHS and k_z dispersion produce effective linewidths which increase rapidly as one moves away from the antinodal point [20]. The present analysis shows that, even if correlation effects were absent, features in the antinodal region would generally be considerably broader than nodal ones, due simply to the effect of k_z dispersion. Caution should be exercised in interpreting differences between theory and experiment in Figs. 1 and 2, since some of these details are sensitive to photon energy and to the precise position of the Fermi energy in relation to the vHS [21].

We have fitted the first-principles FS and band dispersions near E_F in LSCO within the TB model using the form [12]

$$\epsilon_k = -2t(c_x + c_y) - 4t' c_x c_y - 2t''(c_{2x} + c_{2y}) - 2T_z(\vec{k}_\parallel) c_z (c_x - c_y)^2, \quad (1)$$

with $c_i = \cos(k_i a)$ and $c_{2i} = \cos(2k_i a)$, $i = x, y$, $c_z = \cos(k_z c/2)$, and

$$T_z = t_z \cos(k_x a/2) \cos(k_y a/2). \quad (2)$$

The extra angular dependence in Eq. (2) accounts for the staggered stacking of neighboring CuO_2 planes and results in vanishing k_z dispersion along the BZ boundaries. The

parameters which yield a good fit are $t = 0.32$ eV, $t' = -0.25t$, $t'' = -0.02t$, and $t_z = 0.16t$. The latter value should be compared with $t_z = 0.11t$ estimated from transport [22]. In order to simulate the presence of a pseudogap and/or the superconducting gap, the bare bands of Eq. (1) should be replaced by $\epsilon_k \rightarrow \pm E_k$, where $E_k^2 = \epsilon_k^2 + \Delta_k^2$ and $\Delta_k = \Delta_0(c_x - c_y)/2$. In this way a d-wave-like gap with a maximum value of Δ_0 at the M point is produced in the spectrum; we find that Δ_0 grows with underdoping as a pseudogap.

Figure 3 considers the underdoped regime below the superconductor-insulator transition (around $x = 0.06$). Focusing on the experimental [7] spectra first, the half-filled case ($x = 0.0$) in panel (b) is seen to display the presence of the LHB at a binding energy of ≈ 0.5 eV, and little weight around E_F. When the system is doped with a small amount of holes [Fig. 3(a)] substantial weight appears in the midgap spectrum near the M and $(\pi/2, \pi/2)$ points, while the LHB is essentially unchanged. The experimental results of Fig. 3 cannot of course be understood within the conventional LDA-based picture, which fails to produce the insulating state at half-filling. Insight can, however, be obtained via TB models, and accordingly, we have carried out two sets of such calculations: (i) The LHB is fit to TB mean-field computations for a saturated antiferromagnet with Hubbard parameter $U = 6t$, with all other parameters taken directly from the LDA bands. The k_z dispersion is accounted for via the t_z parameter [see Eqs. (1) and (2)]. These TB bands for the two extremal k_z values are given by green lines in Fig. 3. Our parameter values are consistent with earlier data from insulating cuprates based on ARPES [23] and spin wave spectra [24]. (ii) TB calculations (white lines) with the same parameters as those used in the preceding case, except that the Hubbard parameter U is replaced by a d-wave-like pseudogap with $\Delta_0 = 220$ meV at M, which accounts for the presence of such a gap in the experimental spectra at $x = 0.03$.

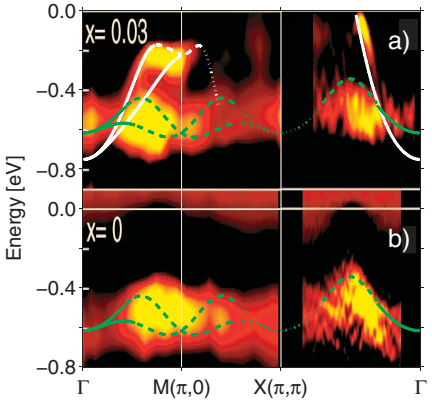

FIG. 3 (color). Tight-binding bands for the AFM (green lines) and d-wave pseudogapped state (white lines) discussed in the text are shown overlayed on experimental second derivative ARPES spectra of Ref. [7] for the undoped ($x = 0.0$) and the lightly doped ($x = 0.03$) LSCO. Data are plotted on a hot color scale where red and black denote lows. Two sets of lines in each case give bands for $k_z = 0$ and $k_z = 2\pi/c$. Different line types give redistributed spectral weights of the uncorrelated states due to the AFM or pseudogap order as follows: 1.0–0.8 (solid lines), 0.8–0.2 (dashed lines), and 0.2–0.01 (dotted lines).

The theoretical bands of Fig. 3 provide a handle on understanding some salient features of the experimental spectra. We consider the LHB along the $\Gamma - M$ and $M - X$ lines first. At both $x = 0$ and $x = 0.03$, the measured LHB is seen to extend over the binding energy range of 0.4–0.8 eV, more or less symmetrically about the M point, at least insofar as its width is concerned. Much of this width can be ascribed to the effect of k_z dispersion, which will cause spectral lines to spread between the boundaries given by the pair of green bands. Note also that the computed LHB is symmetric around M due to the effect of zone folding in the antiferromagnetic (AFM) insulating state. The calculated spectral weights of the green bands are seen to be larger along $\Gamma - M$ compared to the $M - X$ line. The experimental broadening at M cannot be explained by k_z dispersion, but may be due to "hot spot" scattering, since the M point lies on the AFM zone boundary. Along the $\Gamma - X$ line the effect of k_z dispersion is negligible so the substantial observed widths of the LHB must have some other origin.

In contrast, the midgap spectrum of Fig. 3(a) is not symmetric about the M point. The intensity of midgap states cuts off quite abruptly near the M point along the $M - X$ line. This is in accord with the LDA-based bands (white lines), which show little effect of k_z dispersion and also possess little weight to the right-hand side of M. On the other hand, a broad patch of intensity is seen around M extending toward Γ, consistent with the k_z-dispersion boundaries given by the pair of white LDA-based bands. Interestingly, along the $\Gamma - X$ line, the experimental midgap band is quite sharply defined, consistent with the fact that the LDA bands display little k_z-induced broadening.

Taken together, the comparisons of Figs. 1–3 paint a remarkable picture of the way midgap states evolve in LSCO with doping. The fact that the spectrum of the lightly doped insulator in Fig. 2 and along the nodal line in Fig. 3(a) essentially follows the LDA bands indicates that the first midgap states created when holes are added into the Mott insulator mimic metallic states and that a remnant of the quasiparticle (albeit with a small spectral weight) coexists at the Fermi energy with the pseudogapped electronic spectrum [25]. However, it remains unclear how the antinodal spectral weight can be reconciled with the appearance of a pseudogap. Note that in Fig. 2 the quasiparticle displays a substantial spectral weight in the antinodal regions and thus seems to contradict the notion of a "nodal metal" in which the metallic states presumably first form FS arcs around the nodal regions [26]. The fact that hopping appears only weakly renormalized with doping, but that the spectral weight or the intensity of the midgap band decreases with decreasing x, is in the spirit

of a gossamer-type model [9,10]. The presence of a pseudogap near M point will result in predominantly incoherent c-axis transport in the underdoped cuprates [27], whereas there may be coherent c-axis transport in overdoped samples [28]. Certainly, the momentum dependence of the ARPES spectra in the vicinity of E_F are described in considerable detail by the LDA computations as seen from Figs. 1 and 2.

Our study shows that attempts at extracting key information for understanding the mechanism of superconductivity such as self-energies and FS shapes and volumes and their doping dependencies, or to identify signatures of stripe or marginal Fermi liquid physics [29] and other strong correlation effects, must in general take into account the ω- and $\mathbf{k}$-dependent broadening in the ARPES spectra associated with k_z dispersion. For instance, the energy dependent ARPES data of Ref. [29] have been used to adduce evidence of marginal Fermi liquid behavior. Such analysis assumes that the energy (ω) or temperature (T) dependent part of the self-energy is superimposed on a constant (ω and T independent) background, which, however, is found to be strongly dependent on the in-plane momentum. Reference [30] (among others) argues that this constant background is associated with small-angle scattering, since it does not show up in transport measurements. Our preliminary analysis indicates that the k dependence of the ARPES widths arising from the effect of k_z dispersion may in fact explain much of this observed in-plane momentum dependence. More detailed computations and comparisons are, however, necessary to clarify the situation, especially since the effect of k_z-induced broadening also contains energy dependencies.

In conclusion, we have shown with the example of LSCO that effects of k_z dispersion, which have been neglected in most of the existing literature on the cuprates, play a key role in explaining the observed broadening in the ARPES spectra throughout the BZ for both the midgap band as well as the LHB. These results provide a new benchmark for testing strong correlation models of the ARPES spectra. Also, despite the obvious importance of strong correlation effects, the remarkable extent to which the simple LDA-type metallic states describe the dispersion of the midgap spectrum in LSCO, even in the presence of the pseudogap, is an observation calling for theoretical interpretation. We emphasize that the comparisons of Figs. 1 and 2 go well beyond just looking at the dispersion of the bands, but show for the first time that the detailed spectral intensity distribution of the state at the Fermi energy is in remarkable agreement with LDA-based computations, indicating that these states are indeed a remnant of the quasiparticle. Our results provide new constraints for strong correlation models in the cuprates, including insight into the evolution of the midgap states and the pseudogap, and will likely require some revisions of the associated models.

This work is supported by the U.S. Department of Energy Contract No. DE-AC03-76SF00098, and have benefited from the allocation of supercomputer time at NERSC, Northeastern University's Advanced Scientific Computation Center (ASCC), and the Institute of Advanced Computing (IAC), Tampere. We thank X. J. Zhou, T. Yoshida, A. Fujimori, Z. Hussain, and Z. X. Shen, for providing us with the original experimental data of Refs. [4,5,8] so that it could be shown in the color scheme of Figs. 1 and 2.

[1] J. Orenstein and A. J. Millis, Science **288**, 468 (2000).
[2] M. Greiner *et al.*, Nature (London) **415**, 39 (2002).
[3] X. J. Zhou *et al.*, Science **286**, 268 (1999).
[4] X. J. Zhou *et al.*, Phys. Rev. Lett. **86**, 5578 (2001).
[5] T. Yoshida *et al.*, Phys. Rev. B **63**, 220501 (2001).
[6] A. Ino *et al.*, Phys. Rev. B **65**, 094504 (2002).
[7] T. Yoshida *et al.*, Phys. Rev. Lett. **91**, 027001 (2003).
[8] X. J. Zhou *et al.*, Phys. Rev. Lett. **92**, 187001 (2004).
[9] R. B. Laughlin, cond-mat/0209269.
[10] F. C. Zhang, Phys. Rev. Lett. **90**, 207002 (2003).
[11] A. Damascelli *et al.*, Rev. Mod. Phys. **75**, 473 (2003).
[12] A. Bansil *et al.*, Phys. Rev. B **71**, 012503 (2005).
[13] A. Bansil and M. Lindroos, Phys. Rev. Lett. **83**, 5154 (1999).
[14] M. Lindroos *et al.*, Phys. Rev. B **65**, 054514 (2002).
[15] S. Sahrakorpi *et al.*, Phys. Rev. B **68**, 054522 (2003).
[16] A. Bansil *et al.*, Phys. Rev. B **60**, 13 396 (1999).
[17] J. Yu *et al.*, Phys. Rev. Lett. **58**, 1035 (1987).
[18] The projected FSs in Figs. 1 and 2 are integrated over relevant energy windows used in the experimental setup as follows: For $x = 0.06$, $E_F \pm 5$ meV; For $x = 0.15$ and 0.22, the integration is from $E_F - 30$ meV to $E_F + 5$ meV.
[19] Relevant experimental details are $h\nu = 55$ eV and the angle of incidence of light is 7° with the polarization vector being in plane along $[1\bar{1}0]$.
[20] The antinodal point itself is anomalous in that the broadening can be quite small parallel to the BZ boundary (X to M) as seen, for example, from Fig. 2(a).
[21] Although we have focused on emission from the E_F in Figs. 1 and 2, we find that the measured dispersions and the associated widths along the $\Gamma - M$ and $\Gamma - X$ symmetry lines are also described quite well by our computations up to several hundred meV below the E_F.
[22] R. S. Markiewicz, Phys. Rev. B **70**, 174518 (2004).
[23] C. Kusko *et al.*, Phys. Rev. B **66**, 140513(R) (2002).
[24] N. M. R. Peres and M. A. N. Araújo, Phys. Status Solidi A **236**, 523 (2003).
[25] ARPES studies of $Ca_2CuO_2Cl_2$ reveal a similar situation [K. M. Shen *et al.*, Phys. Rev. Lett. **93**, 267002 (2004)].
[26] X.-G. Wen and P. A. Lee, Phys. Rev. Lett. **76**, 503 (1996).
[27] J. H. Kim *et al.*, Physica (Amsterdam) **247C**, 297 (1995).
[28] Coherent 3D coupling has been reported recently in an overdoped Tl cuprate by N. E. Hussey *et al.*, Nature (London) **425**, 814 (2003).
[29] T. Valla *et al.*, Nature (London) **417**, 627 (2002).
[30] E. Abrahams and C. M. Varma, Proc. Natl. Acad. Sci. U.S.A. **97**, 5714 (2000).